Surface-enhanced mid-infrared spectroscopy using a quantum cascade laser

Anton Hasenkampf,[1] Niels Kröger,[1] Arthur Schönhals,[1] Wolfgang Petrich,[1] and Annemarie Pucci[1]*

[1] *University of Heidelberg, Kirchhoff Institute for Physics, Im Neuenheimer Feld 227, 69120 Heidelberg, Germany*
**pucci@kip.uni-heidelberg.de*

Abstract: We report on the successful measurement of surface-enhanced infrared vibrational spectra from a few nanometer thick organic semiconductor layers on samples with resonant plasmonic nanoantennas arranged in arrays. For the first time, a setup with a tunable quantum cascade laser as the light source in mid-infrared range is used. The combination of the quantum cascade laser with a microbolometer array for infrared light allows to map an area 2.8 × 3.1 mm^2 with a spatial resolution of about 9 μm, a bandwidth from 1170 to 1300 cm^{-1}, and a spectral resolution of 2.5 cm^{-1} within only five minutes versus 16 hours using a conventional FTIR micro-spectrometer. We present a quantitative comparison of the experimental results from the setup with the quantum cascade laser with those from the FTIR micro-spectrometer.

OCIS codes: (300.6340) Spectroscopy, infrared; (240.6680) Surface plasmons; (250.5403) Plasmonics; (140.3070) Infrared and far-infrared lasers

References and links

1. C. Huck, F. Neubrech, J. Vogt, A. Toma, D. Gerbert, J. Katzmann, T. Härtling, and A. Pucci, "Surface-enhanced infrared spectroscopy using nanometer-sized gaps," ACS Nano **8**(5), 4908–4914 (2014).
2. F. Neubrech, A. Pucci, T. W. Cornelius, S. Karim, A. García-Etxarri, and J. Aizpurua, "Resonant plasmonic and vibrational coupling in a tailored nanoantenna for infrared detection," Phys. Rev. Lett. **101**(15), 157403 (2008).
3. R. Adato, A. A. Yanik, J. J. Amsden, D. L. Kaplan, F. G. Omenetto, M. K. Hong, S. Erramilli, and H. Altug, "Radiative engineering of nanoantenna arrays for ultra-sensitive vibrational spectroscopy of proteins," Proc. SPIE **7757**, 77571W (2010).
4. F. Neubrech, S. Beck, T. Glaser, M. Hentschel, H. Giessen, and A. Pucci, "Spatial extent of plasmonic enhancement of vibrational signals in the infrared," ACS Nano **8**(6), 6250–6258 (2014).
5. H. Aouani, M. Rahmani, H. Šípova, V. Torres, K. Hegnerová, M. Beruete, J. Homola, M. Hong, M. Navarro-Cía, and S. A. Maier, "Plasmonic nanoantennas for multispectral surface-enhanced spectroscopies," J. Phys. Chem. C **117**(36), 18620–18626 (2013).
6. F. Neubrech and A. Pucci, "Plasmonic enhancement of vibrational excitations in the infrared," IEEE J. Sel. Top. Quantum Electron. **19**(3), 4600809 (2013).
7. R. Bardhan, N. K. Grady, J. R. Cole, A. Joshi, and N. J. Halas, "Fluorescence enhancement by Au nanostructures: nanoshells and nanorods," ACS Nano **3**(3), 744–752 (2009).
8. A. Kinkhabwala, Z. Yu, S. Fan, Y. Avlasevich, K. Müllen, and W. E. Moerner, "Large single-molecule fluorescence enhancements produced by a bowtie nanoantenna," Nat. Photonics **3**(11), 654–657 (2009).
9. H. Aouani, H. Šípová, M. Rahmani, M. Navarro-Cia, K. Hegnerová, J. Homola, M. Hong, and S. A. Maier, "Ultrasensitive broadband probing of molecular vibrational modes with multifrequency optical antennas," ACS Nano **7**(1), 669–675 (2013).
10. S. Cataldo, J. Zhao, F. Neubrech, B. Frank, C. Zhang, P. V. Braun, and H. Giessen, "Hole-mask colloidal nanolithography for large-area low-cost metamaterials and antenna-assisted surface-enhanced infrared absorption substrates," ACS Nano **6**(1), 979–985 (2012).
11. C. D'Andrea, J. Bochterle, A. Toma, C. Huck, F. Neubrech, E. Messina, B. Fazio, O. M. Maragò, E. Di Fabrizio, M. Lamy de La Chapelle, P. G. Gucciardi, and A. Pucci, "Optical nanoantennas for multiband surface-enhanced infrared and Raman spectroscopy," ACS Nano **7**(4), 3522–3531 (2013).
12. K. Kneipp, Y. Wang, H. Kneipp, L. T. Perelman, I. Itzkan, R. R. Dasari, and M. S. Feld, "Single molecule detection using surface-enhanced Raman scattering (SERS)," Phys. Rev. Lett. **78**(9), 1667–1670 (1997).
13. J. Theiss, P. Pavaskar, P. M. Echternach, R. E. Muller, and S. B. Cronin, "Plasmonic nanoparticle arrays with nanometer separation for high-performance SERS substrates," Nano Lett. **10**(8), 2749–2754 (2010).

#226535 - $15.00 USD Received 7 Nov 2014; revised 7 Jan 2015; accepted 2 Feb 2015; published 24 Feb 2015

14. S. Nie and S. R. Emory, “Probing single molecules and single nanoparticles by surface-enhanced Raman scattering,” Science **275**(5303), 1102–1106 (1997).
15. B. Fazio, C. D’Andrea, F. Bonaccorso, A. Irrera, G. Calogero, C. Vasi, P. G. Gucciardi, M. Allegrini, A. Toma, D. Chiappe, C. Martella, and F. Buatier de Mongeot, “Re-radiation enhancement in polarized surface-enhanced resonant Raman scattering of randomly oriented molecules on self-organized gold nanowires,” ACS Nano **5**(7), 5945–5956 (2011).
16. M. J. Weida and B. Yee, “Quantum cascade laser based replacement for FTIR microscopy”, Proc. SPIE **7902**, 79021C (2011).
17. N. Kröger, A. Egl, M. Engel, N. Gretz, K. Haase, I. Herpich, S. Neudecker, A. Pucci, A. Schönhals, and W. Petrich, “Rapid hyperspectral imaging in the mid-infrared,” Proc. SPIE **8939**, 89390Z (2014), doi:10.1117/12.2041988.
18. T. Glaser, S. Beck, B. Lunkenheimer, D. Donhauser, A. Köhn, M. Kröger, and A. Pucci, “Infrared study of the MoO_3 doping efficiency in 4,40-bis(N-carbazolyl)-1,10-biphenyl (CBP),” Org. Electron. **14**(2), 575–583 (2013).
19. N. Kröger, A. Egl, M. Engel, N. Gretz, K. Haase, I. Herpich, B. Kränzlin, S. Neudecker, A. Pucci, A. Schönhals, J. Vogt, and W. Petrich, “Quantum cascade laser-based hyperspectral imaging of biological tissue,” J. Biomed. Opt. **19**(11), 111607 (2014).

1. Introduction

Surface-enhanced infrared (IR) absorption (SEIRA) spectroscopy [1–6] is developing towards a standard technique for the detection of molecular vibrations with improved sensitivity. On metal nanostructures, the main origin of the signal enhancement in SEIRA is the strong near-field at plasmonic resonances. This plasmonic attribute has been proven many times, for example, in surface-enhanced fluorescence [7,8], surface-enhanced infrared absorption [1–6, 9–11] (SEIRA), and surface-enhanced Raman spectroscopy (SERS) [12–15]. A rod shaped nanostructure, a nanoantenna, can enhance the SEIRA signal by up to five orders of magnitude [2]. If arranged in a homogeneous array, these nanoantennas possess excellent far-field signals that can be measured with a FTIR spectrometer. FTIR spectrometers typically use either one of the two mid-infrared (MIR) light sources, a globar or a synchrotron. Both sources offer a broad spectrum in the IR, but have a low spectral power density [16] compared to quantum cascade lasers (QCL). Recent improvements and developments have now enabled the use of a QCL as a light source also in MIR microscopy [17]. In this contribution we present example measurements of a SEIRA signal from a thin layer of 4,4'-bis(N-carbazolyl)-1,1'-biphenyl (CBP) molecules with a microscope setup that uses a QCL as the MIR light source [17]. The SEIRA signal is enhanced by means of resonant rod shaped gold nanoantennas arranged in arrays. For comparison, measurements of the same samples were performed with a conventional FTIR micro-spectrometer (Bruker Hyperion 1000) which uses a globar light source. We discuss both measurements and compare the results, demonstrating the superior acquisition time advantage of the QCL system - with a comparable spatial and spectral resolution.

2. Experimental

The gold nanoantennas were fabricated by electron beam lithography (EBL) on a CaF_2 (100) substrate using a Leo 1530 scanning electron microscope (SEM) equipped with an Elpy Quantum nanopattern generator. The substrate was cleaned in an ultrasonic bath of acetone and isopropanol. Then a layer of 80 nm polymethyl methacrylate (PMMA) was spin coated at 2500 rpm for 90 seconds. An additional layer of 10 nm aluminum was evaporated thermally in order to avoid charging. The nanopatterning of the sample was performed with 15 kV acceleration voltage and an e-beam current of 13 pA. After the nanopatterning, the alumina layer is removed with sodium hydroxide (NAOH). The nanopatterns are developed using a mixture of methyl isobutyl ketone isopropyl alcohol (IPA), isopropanol, and ethylmethylketone at the ratio of 100:300:6. Next, a 55 nm gold layer on top of a 5 nm chrome adhesive layer was evaporated at room temperature. The remaining PMMA is removed with acetone. A SEM image of an array can be seen in Fig. 1.

#226535 - $15.00 USD Received 7 Nov 2014; revised 7 Jan 2015; accepted 2 Feb 2015; published 24 Feb 2015

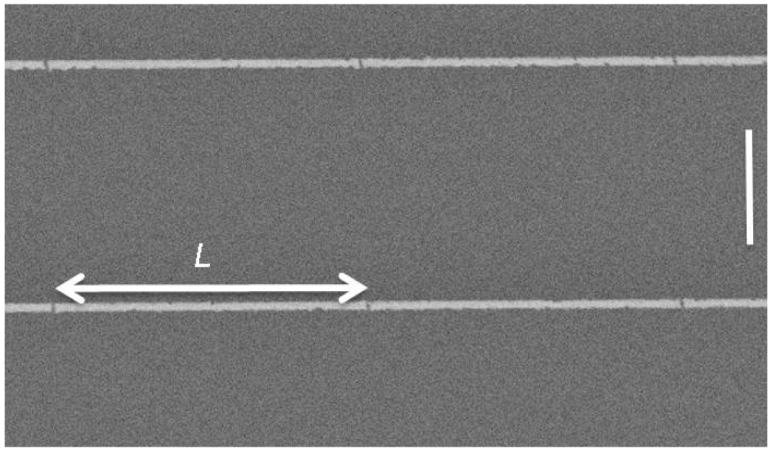

Fig. 1. SEM image of a typical SEIRA active nanoantenna array. The array consists of nanoantennas, with length L = 2.8 µm, gaps of 50 nm in longitudinal direction and of 2 µm in transverse direction, respectively. The vertical scale bar is 1 µm long.

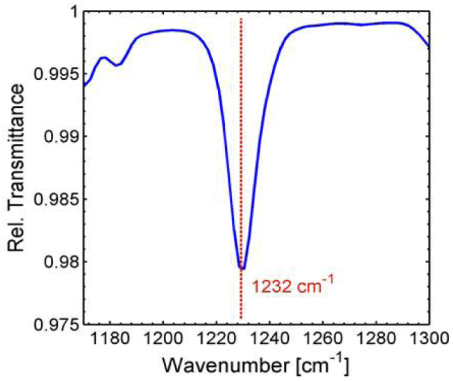

Fig. 2. Measured transmittance spectrum of 68 nm CBP on silicon. The band in the range of the QCL setup is marked in red.

The nanoantennas have all the same width (60 nm) and height (5 nm chrome + 55 nm gold). Multiple nanoantennas were arranged into rectangular arrays of fields of distinct geometric features. The length L and the longitudinal gap size vary from field to field (L = 3000, 2800, 2600 nm for one sample, L = 2400, 2200, 2000, 1800 nm for the other, and 50, 30 and 20 nm for the gap size, respectively). The size of the arrays is 100 × 100 µm^2 and the distance between two antennas in the transverse direction is 2 µm for all arrays. The various lengths L of the nanoantennas lead to various plasmonic resonances in the range of the CBP fingerprint vibrations. In preparation of the SEIRA measurements, the whole sample was cleaned in oxygen plasma (150 W, 10 min, 0.4 bar). The CBP was evaporated onto the cleaned arrays under ultrahigh vacuum conditions. Among others, CBP possesses a strong vibrational band at a wavenumber 1230 cm^{-1}, see Fig. 2, which is within the tuning range of the QCL. The CBP molecules on the surface of the sample are mainly bound by Van der Waals interaction and form an amorphous, almost homogeneous and isotropic layer (root-mean-square surface roughness below 1 nm) on CaF_2 and gold. The layer is stable under standard ambient temperature and pressure conditions for several weeks. Deposition rates were measured with a quartz crystal microbalance and were used for the thickness determination (assuming constant evaporation). Two layer thicknesses were inspected; ca. 1nm (± 50%) and 5nm (± 10%). A reference spectrum of CBP was measured using a Bruker

#226535 - $15.00 USD Received 7 Nov 2014; revised 7 Jan 2015; accepted 2 Feb 2015; published 24 Feb 2015

Vertex 80v FTIR spectrometer with a globar light source and a mercury cadmium telluride detector. The whole beam path was evacuated during that measurement. The CBP reference spectrum was recorded with a resolution of 4 cm^{-1} and 200 scans [18]. The infrared spectroscopy of the arrays was performed with two light sources, the QCL and the globar. Concerning the delivered power per 1 cm^{-1} bandwidth, the typical infrared QCL power is up to nine orders of magnitude better, but it is lowered by the used beam shaping optics. Our homemade QCL set-up is shown in Fig. 3.

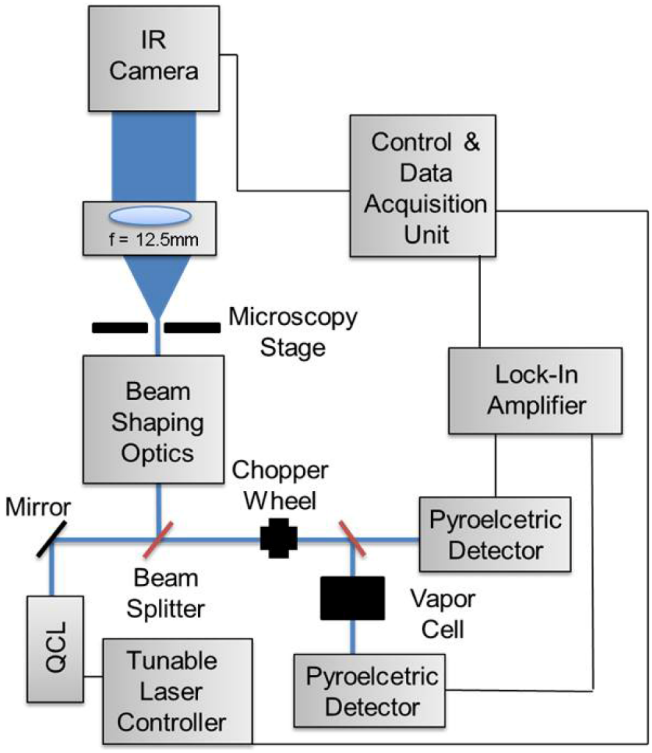

Fig. 3. Schematic of the QCL microscope setup. A QCL (1170-1300 cm^{-1}) is combined by a non-polarizing beam splitter (NPBS). The magnification is determined by the lens (f = 12.5 mm for 4:1) in front of the IR camera (microbolometer FPA). The sample illumination can be matched to the desired field of view by adjustable beam shaping optics. Laser power and wavelength can be monitored parallel to micro-spectroscopy by measuring the transmittance through a thermally stabilized gas cell filled with ethanol and/or water vapor [17].

Here, a QCL (type ÜT-8, Daylight Solutions Inc., San Diego, USA) with the tuning range from 1140 –1440 cm^{-1} was used. The whole setup was purged with dry air. The sample is illuminated with the QCL and the imaging is performed with an IR camera using a micro-bolometer focal plane array detector (FPA detector) with 640×480 pixels. The average laser power in the sample plane is below 10 mW. The pulsed Laser was running at 10% duty cycle, resulting in a maximum peak power of 100 mW in the sample plane, or roughly 0.3 µW per pixel of the micro-bolometer focal plane array detector. At these power levels, no damage was observed. The sensitivity of the camera covers a spectral range from 1170 to 1300 cm^{-1}. The decrease in output power towards the limits of the tuning range of the QCL reduces the effective spectral range.

#226535 - $15.00 USD Received 7 Nov 2014; revised 7 Jan 2015; accepted 2 Feb 2015; published 24 Feb 2015

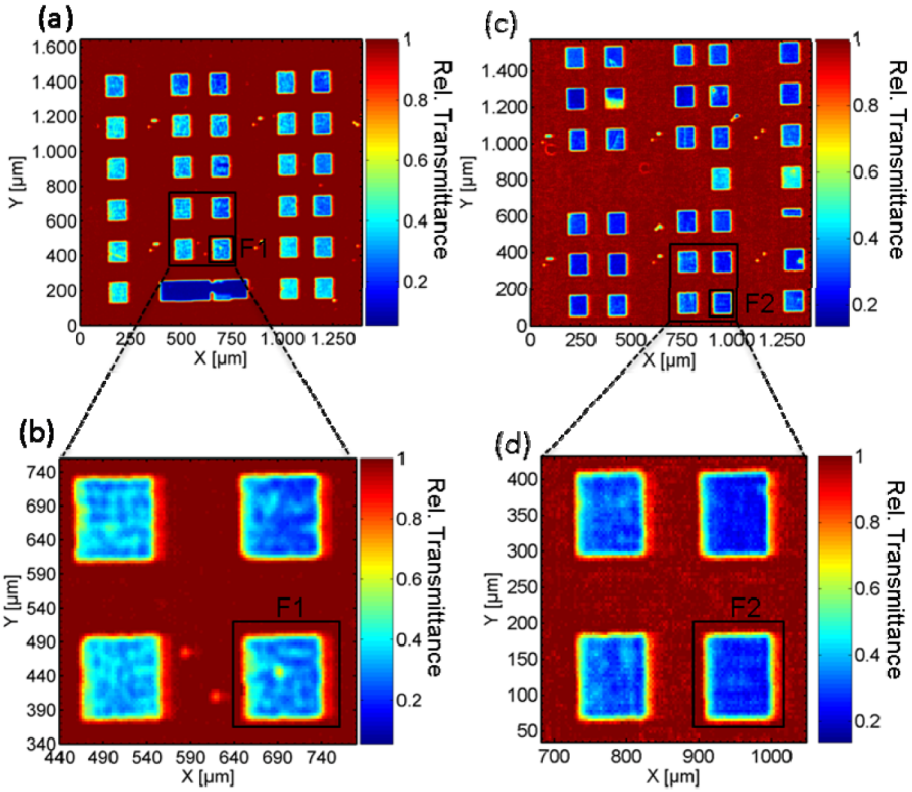

Fig. 4. Transmittance maps at 1230 cm^{-1} obtained with the QCL-microscope of samples with antenna arrays and 1 nm CBP, (a) and (b), and 5 nm, (c) and (d), respectively. The different colors correspond to the intensity in relative transmittance of the nanoantenna arrays in the different areas of the samples. The size of the images for (a) and (c) is about 1.4 mm^2. The spatial resolution is about 9 µm. The differences of the arrays within each transmittance map can be clearly recognized. The images (b) and (d) show zooms into the transmittance maps (a) and (d). The detailed structure of the arrays can be recognized and thus also the quality of the fabricated arrays. The measurement with the QCL microscope setup took ca. 5 minutes. The field F1 and F2 (see also Fig. 5) are marked.

The microscope images have been captured with the f = 12.5 mm lens, resulting in a nominal magnification of 4:1 and a projected pixel size of 7.3 µm with a total field of view of 2.8 x 3.1 mm^2. Spatial resolution can be enhanced with special oversampling (see appendix). Thus, a projected pixel size of 3.65 µm and a spatial resolution of 9 ± 1.8 µm can be achieved [19]. Spatial oversampling was used for all the measurements performed with the QCL setup in this paper. IR spectra were taken by tuning the QCL over its spectral range (sweep-scan). This allows a time-dependent spectral measurement with the micro-bolometer array. A sweep-scan over the whole spectral range of the QCL takes about 12 seconds. When using spatial oversampling, four transmittance spectra plus one reference are needed. This is done 5 times for the improvement of the signal-to-noise ratio. In total this takes about 5 × 60 s = 300 s = 5 minutes. Since the laser is already linearly polarized, the spectra shown in the Figs. 4-8 for polarized light were taken without an additional polarizer. The laser-light polarization was parallel to the long axis of the nanostructures, so that the fundamental antenna resonance could be excited [2,11]. The typical standard deviation of the 100% line of single pixels for the chosen parameters of the QCL setup is below 1% [17] (signal-to noise ratio S/N >100). QCL based IR spectra are shown as after averaging over the pixels of a cluster, see appendix. With the globar, the transmittance measurements of the arrays were performed by means of a conventional FTIR microscope (Bruker IRscope II, Bruker Optics GmbH, Ettlingen,

#226535 - $15.00 USD Received 7 Nov 2014; revised 7 Jan 2015; accepted 2 Feb 2015; published 24 Feb 2015

Germany). A Schwarzschild objective with a numerical aperture NA = 0.5 was used together with a circular aperture with the diameter of 50.4 µm for the measurements of spectra and with 8.3 µm in diameter for microscopic images. The FTIR set-up was purged with dry air.

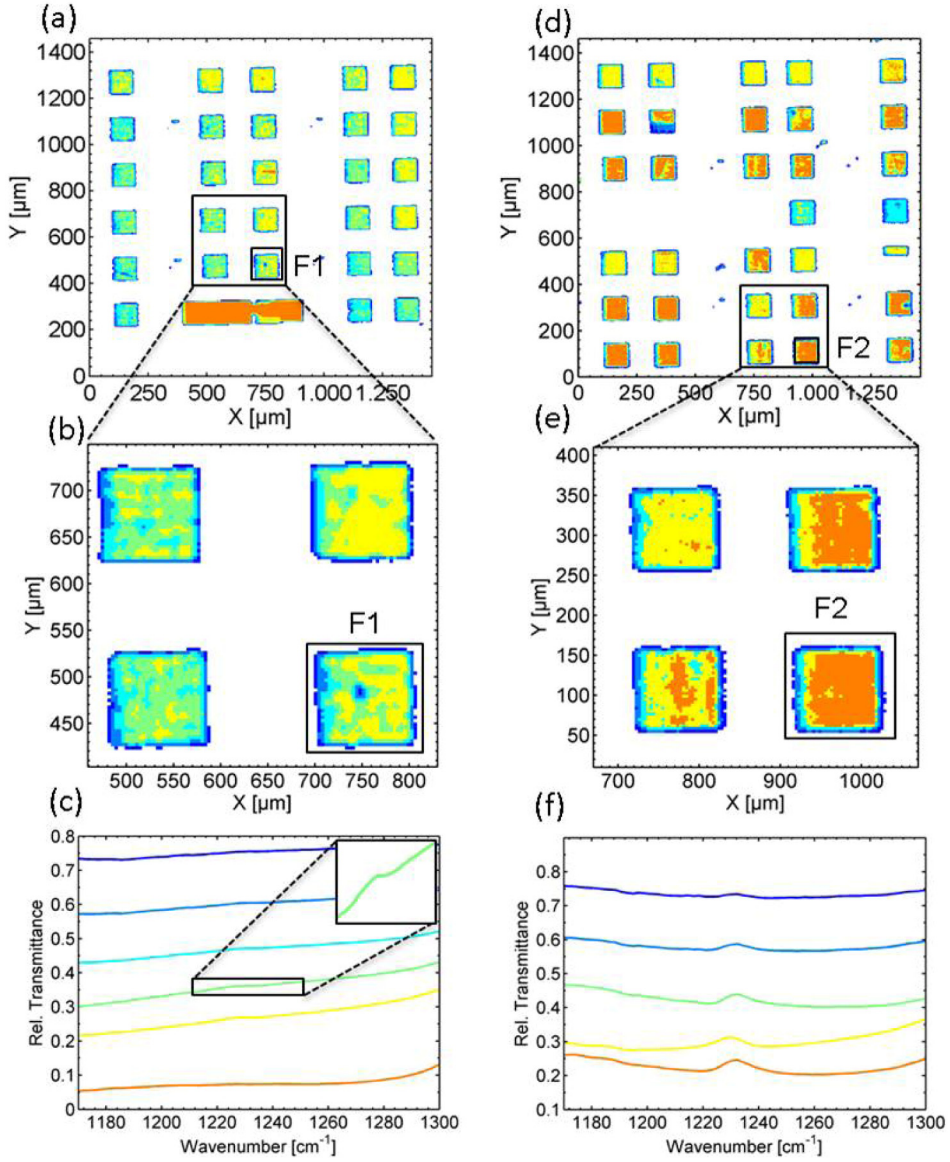

Fig. 5. Cluster maps of obtained hyperspectral measurements with the QCL-microscope (a), (b) and (d), (e) and IR spectra of the individual clusters in (c) and (f) of samples with antenna arrays and 1 nm CBP ((a)-(c)) and 5 nm ((d)-(f)), respectively. The spectral resolution is 2.5 cm^{-1} and the gained spectral data covers the range from 1170 to 1300 cm^{-1}. (b) and (e) show zooms into the cluster maps of (a) and (d). Two arrays are marked as field 1 (F1) and field 2 (F2), their further enlargements are shown in Fig. 5 and Fig. 6(a). The different colors in the cluster maps correspond to different clusters. Their mean spectra are shown in (c) (including a zoom to the CBP signal) and (f). The mean spectrum of a cluster is determined by averaging over the individual spectra of the pixels.

The spectral measurements were carried out with a FTIR spectrometer with a liquid-N_2-cooled mercury–cadmium telluride detector. A polarizer was inserted in the optical beam path

#226535 - $15.00 USD Received 7 Nov 2014; revised 7 Jan 2015; accepted 2 Feb 2015; published 24 Feb 2015

in order to linearly polarize the light with the electric field parallel to the nanoantennas. Transmittance spectra of the arrays and of the reference spectra were captured by acquisition of 100 scans (within 92 s) in a spectral range from 800 to 8000 cm^{-1} and measured with a resolution of 4 cm^{-1}. For these conditions and the 50.4 µm - aperture, the deviations from the 100% line in the range of the investigated CBP band are below 0.15% (S/N > 600). For a further improved S/N, the FTIR spectra of the CBP covered arrays and their reference spectra were averaged over 10 measurements. The reference for the transmittance measurements of the CBP covered arrays was taken on the CBP covered CaF_2 substrate in a distance of 0.5 mm away from the measured array.

3. Results and discussion

Relative transmittance measurements of two samples that have both a CBP layers on top with different thickness are shown in Fig. 4. The individual colors correspond to the different intensities of the transmittance signal at 1230 cm^{-1}, the CBP vibrational band. The size of the exhibited area is around 1.4 mm^2. Further data points have been excluded, because they only show the surface of the sample without arrays on it. The structures on the samples can be clearly distinguished from the background in Fig. 4(a) and 4(c). Figure 4(b) and 4(d) show enlarged views of a small region of the image. These enlargements required no additional measurements and make the detailed structure of the individual array visible. The detailed structure provides an insight into the homogeneity and quality of the manufactured arrays. Cluster maps of transmittance measurements of the two samples that have both a CBP layers on top, but with different thickness, are shown in Fig. 5. These images were calculated from the spectral data using a method called cluster mapping (see appendix) with the MATLAB software (The MathWorks GmbH). Figure 5(b) and 5(e) present zooms to small regions of the images. The clusters in Fig. 5(a) and 5(d) can be recognized by their individual color. The spectra corresponding to the individual clusters and colors can be seen in Fig. 5(c) and 5(f). The cluster mean spectra are calculated by averaging up spectra of the individual pixels of a cluster. The transmittance spectra in Fig. 5(f) show an increase in transmission at the vibrational band of CBP. This is a typical SEIRA feature, see below.

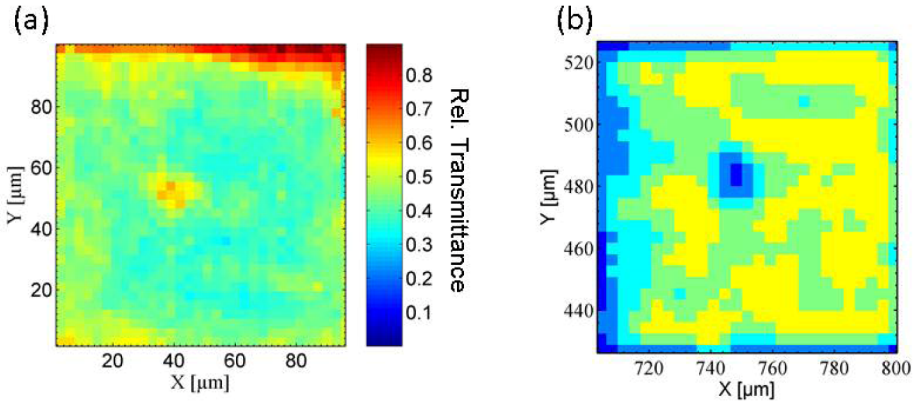

Fig. 6. Comparison between the images of the example of array F1 from Fig. 5(a) using (a) the FTIR and (b) QCL microscope. The analyzed spectrum covers the range from 1170 to1300 cm^{-1} in both images. (a) The FTIR measurement's color map: The different colors correspond to the intensity in relative transmittance of the nanoantennas in the different areas of the field. Their value is explained with the color bar. (b) Enlargement from Fig. 5(a) into the same field. Both maps (a) and (b) show the same distinct feature in their middle, which can be identified as an area with a lower transmittance.

Figure 6(a) depicts an array map taken with the FTIR micro-spectroscopy setup. The array corresponds to field F1 in Fig. 5(a) and 5(b). The individual data points of the image

#226535 - $15.00 USD Received 7 Nov 2014; revised 7 Jan 2015; accepted 2 Feb 2015; published 24 Feb 2015

correspond to relative transmittance measurement taken with the FTIR. The array was scanned in 3 µm steps horizontally and vertically, with 33 steps in each direction. The aperture had a diameter of 8.3 µm. With the small aperture and for the used 100 scans, the deviations from the 100% line are below 1.6% (S/N > 60). The analysed spectal data for the color coded map covers the range from 1170 to 1300 cm^{-1}. The individual colors correspond to the different intensities of the transmittance signal integrated over this spectral range. The map shows a distinctive feature in the middle which can be identified as an area with low transmittance. The measurements for that image took about 16 hours. Taking an image from the whole sample with all the arrays with the FTIR micro-spectroscopy setup (with the same resolution as the QCL-based setup and S/N ca. 60) would take more than a full month of continuous FTIR mapping. Imaging the whole sample with the QCL setup took only five minutes. However, the QCL spectral range is much smaller and needs to be tuned to the excitations of interest. Figure 6(b) zooms into field F1 from Fig. 5(a). The resolution allows for observing individual pixels and so the detailed structure of the array. Like in the FTIR measurement, this image shows an area of low transmittance in its center. The good correspondence of the two measurements makes clear that the spatial information about the properties of the sample from The good correspondence of the two measurements makes clear that the spatial information about the properties of the sample from the measurement with QCL-based microscope is correct.

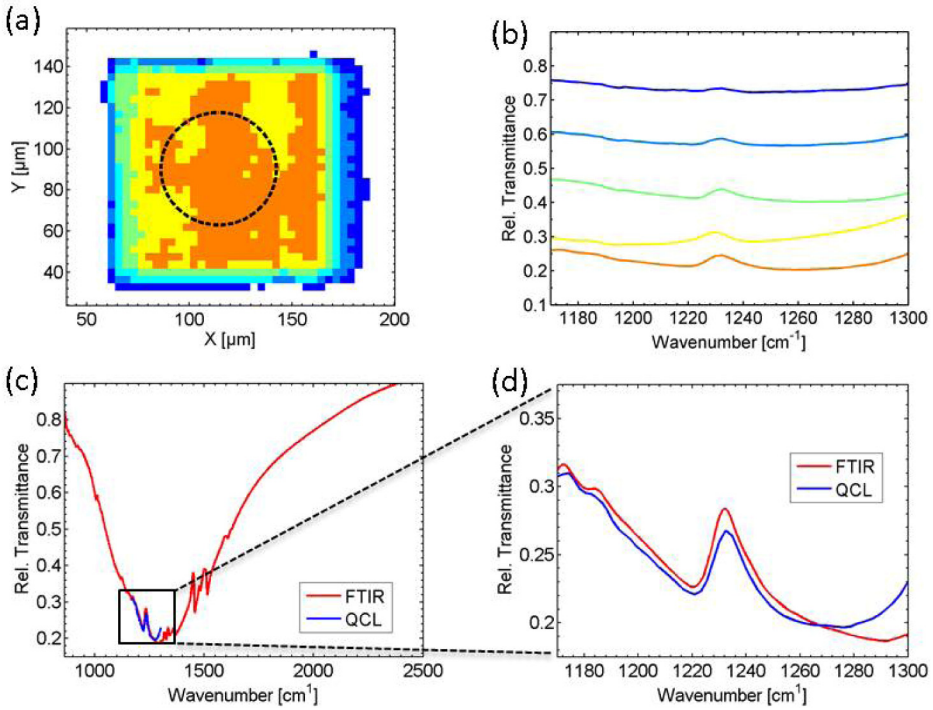

Fig. 7. Comparison between spectra from array F2 (a) taken with the QCL and the FTIR set up. (b) shows the spectra as they are used for the color code of the cluster maps in (a). The measurement with the FTIR is done in the middle of the 100 × 100 µm array with a 50.4 µm aperture. The area has been marked with a dotted black line in (a). The spectral bandwidth covers the range from 800 to 8000 cm^{-1} (FTIR) and from 1170 to 1300 cm^{-1} (QCL), respectively. (c) Relative transmittance of the array measured with both the FTIR and QCL-setup. Only the marked area of (a) is used for comparison. (d) Zoom to the spectral region between 1170 and 1300 cm^{-1} of (c). Both spectra show the CBP mode at 1230 cm^{-1} on the antennas resonance background.

#226535 - $15.00 USD Received 7 Nov 2014; revised 7 Jan 2015; accepted 2 Feb 2015; published 24 Feb 2015

Figure 7 compares the FTIR and the QCL measurements from field F2 of Fig. 5(d). Figure 7(a) shows the cluster map from field F2. The nanoantennas in this array have the length of 2800 nm, the longitudinal gap size between two of them is 25 nm. The relative transmittance measurements of the yellow and orange cluster are nearly uniform. This indicates that the fabrication of the array and the homogeneous covering with the CBP were successfully done. The black dotted line in Fig. 7(a) includes the area of the array that was selected with the aperture for the integral FTIR measurement. The shown pixels in this area correspond to the QCL based spectra of Fig. 7(c) and 7(d). Figure 7(c) and (d) compare the relative transmittance spectra from the FTIR microscopic measurement and the QCL based one. For the FTIR spectrum, the commercial FTIR microscope with an aperture of 50.4 µm was used. No information about homogeneity was obtained from this integral measurement. Both kinds of relative transmittance spectra are indeed very similar in spectral information and S/N. The CBP mode at 1230 cm^{-1} is clearly visible in both the FTIR and QCL spectrum of the relative transmittance (that is already normalized to the spectrum of the CBP layer on CaF_2). The shape of the mode at 1230 cm^{-1} clearly is not that of a typical Lorentzian absorption band. It is a Fano-type line shape due to the resonant plasmonic coupling of the vibrational dipoles with their frequency at the plasmonic resonance [2, 6]. This coupling is analogous to the quantum mechanical interaction between a continuum of states and a discrete state, which produces Fano profiles.

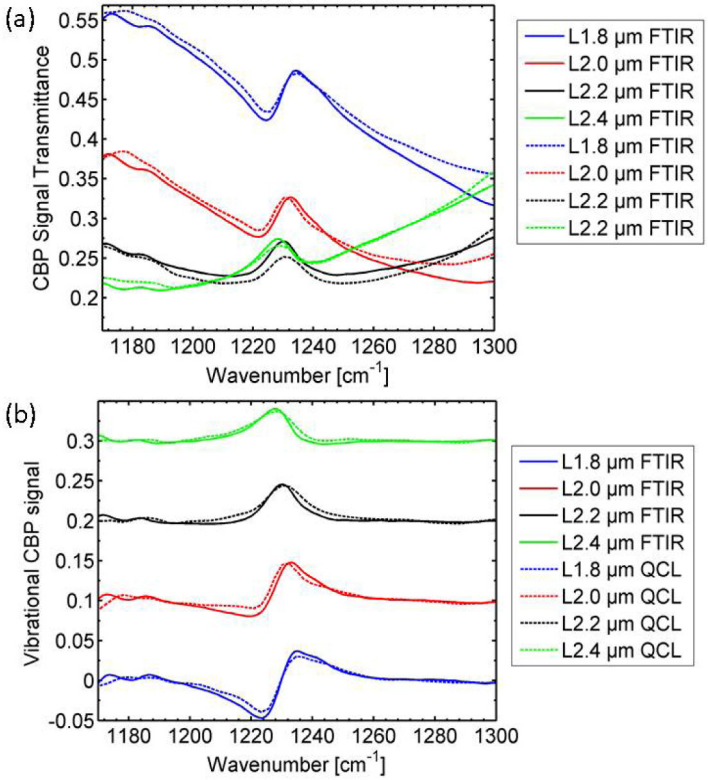

Fig. 8. The relative transmittance spectra (a) and the baseline corrected CBP molecular signals (b) for several arrays with different length *L* (as given) taken with the FTIR and QCL from the sample with 5 nm CBP on top. The individual measurements in (b) have been vertically shifted against each other. The CBP mode at 1230 cm^{-1} has clearly the same characteristics in both the FTIR spectrum and QCL spectrum. For the baseline correction, see [1] and its Supporting Information.

#226535 - $15.00 USD Received 7 Nov 2014; revised 7 Jan 2015; accepted 2 Feb 2015; published 24 Feb 2015

These profiles go from a dip to an asymmetric line depending on the matching between the antenna resonance and the molecular vibrations. Such SEIRA signals appear only if the molecules are at sites with resonant near-field enhancement. For our sample with only 1 nm average CBP thickness, the nearly invisible SEIRA signal indicates that there are probably less molecules at the nanoantennas' apexes due to the thickness inhomogeneity for such low coverage. Figure 8(a) and 8(b) present the transmittance spectra from several arrays with different lengths 2.4, 2.2, 2.0, and 1.8 μm (meaning different detuning of the plasmonic resonance) and the longitudinal gap size of 50 nm. The continuous lines are measurements performed with the FTIR micro-spectrometer and the dashed lines belong to the spectra measured with the QCL set up. The two kinds of spectra show a very good accordance in relative transmittance for all the inspected antenna lengths. The baseline corrected vibrational CBP signals in Fig. 8(b) nicely show the various Fano-type line shapes due to the different detuning of the plasmonic resonance and the molecular vibration [2, 6, 11].

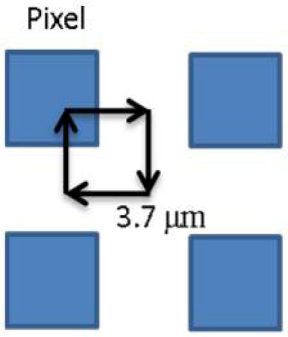

Fig. 9. A schematic of oversampling. The arrows show the movement of the sample. The blue dots are the pixel.

4. Conclusions

We have demonstrated that it is possible and even very advantageous to use a QCL-based setup for SEIRA measurements on plasmonic nanostructure arrays. Various arrays tuned to different resonance frequencies and distributed over a large sample area were simultaneously measured with a QCL-based setup, whereas with FTIR micro-spectroscopy each array had to be measured separately. The analyzed spectral data from the arrays showed the same features for the nanoantenna resonance and the SEIRA signal of CBP when comparing the FTIR to the QCL based data. The image acquired with the QCL additionally contained spatial information about the properties and the quality of the different arrays, for example, the homogeneity of an array or the coating quality in accord to the information of an image that was acquired with a much more time consuming FTIR-based measurement. The results thus prove that fast SEIRA sensing is possible with QCL microscopy.

5. Appendix

5.1. Spatial oversampling

Oversampling is a technique that is used here with the QCL setup in order to achieve a better resolution. The pixel pitch of the microbolometer array is 7.3±0.2 μm. The pixel pitch is the lateral displacement of the individual pixels. In an oversampling measurement, the sample is moved in four steps (like on a square, see Fig. 9) and the measurements are done at the corners. Each step moves 3.7 μm, half of the pixel pitch. Since the steps are smaller than the pixel pitch, the pixels move with each step in a new measurement area. This measurement technique enables to gain additional data points in an area where the pixels normally do not provide information and improve this way the resolution.

#226535 - $15.00 USD Received 7 Nov 2014; revised 7 Jan 2015; accepted 2 Feb 2015; published 24 Feb 2015

5.2. Cluster mapping

Cluster mapping is data-analysis technique. It can be used to analyze the spectra of the individual pixels from a hyperspectral image and to obtain a color-coded image based on spectral similarities among the individual spectra. The pixels are sorted into groups according to the similarity of the respective spectra. These groups are called clusters. The spectrum of a cluster is determined by averaging the spectra of all pixels in the cluster. An individual color is assigned to each cluster. This creates an image that is shown together with the spectra of the individual clusters in Fig. 4-6. In this works, the "k-means" clustering algorithm from the MATLAB statistics toolbox was used.

Acknowledgments

We thank Dr. Tobias Glaser, Sabina Hillebrandt, and Johannes Zimmermann for evaporating CBP on the samples and that it could be done in the InnovationLab GmbH Heidelberg with the facility of the MESOMERIE-BMBF project (FKZ 13N10724). Anton Hasenkampf and Arthur Schönhals acknowledge support from the Heidelberg Graduate School of Fundamental Physics.

Competing interests

The authors have no competing financial interests. In addition to his affiliation with the Kirchhoff-Institute for Physics, W.P. is an employee of Roche Diagnostics GmbH, Mannheim, Germany.

#226535 - $15.00 USD Received 7 Nov 2014; revised 7 Jan 2015; accepted 2 Feb 2015; published 24 Feb 2015